Atmos. Chem. Phys. Discuss., 5, 8209–8232, 2005
www.atmos-chem-phys.org/acpd/5/8209/
SRef-ID: 1680-7375/acpd/2005-5-8209
European Geosciences Union

Atmospheric Chemistry and Physics Discussions

A redistribution of water due to pileus cloud formation near the tropopause

T. J. Garrett[1], C. Liu[1], J. Dean-Day[2], B. K. Barnett[3], G. G. Mace[1], D. G. Baumgardner[5], C. R. Webster[6], T. P. Bui[2], and W. G. Read[6]

[1]Department of Meteorology, University of Utah, Salt Lake City, UT, USA
[2]Atmospheric Chemistry and Dynamics Branch, NASA Ames Research Center, Moffett Field, CA, USA
[3]WB-57 Program Office, NASA Johnson Space Center,Ellington Field, Houston, Texas, USA
[5]Universidad Nacional Autonoma de Mexico, Mexico City, Mexico
[6]Jet Propulsion Laboratory, 4800 Oak Grove Drive, Pasadena, CA, USA

Received: 6 July 2005 – Accepted: 18 July 2005 – Published: 8 September 2005

Correspondence to: T. Garrett (tgarrett@met.utah.edu)

Abstract

Thin stratiform clouds called pileus can form in the earth's atmosphere when humid air is lifted above rising convection. In the lower troposphere pileus lifetimes are short, so they have been considered little more than an attractive curiosity. This paper describes pileus cloud forming near the tropopause at low-latitudes, and discusses how they may be associated with a redistribution of water vapor and ice at cold temperatures.

1 Introduction

At low latitudes, the tropopause transition layer (TTL) extends from approximately 14 to 18 km altitude. It is characterized by high vertical gradients in water concentration and a local minimum in temperature. The mechanisms governing distributions of water vapor and ice in the TTL have attracted considerable interest. This is primarily because these species contribute to the planetary greenhouse mechanism by strongly absorbing terrestrial radiation at temperatures typically 100 K colder than the surface, thereby limiting its loss to space.

This paper attempts to describe a process that demonstrably repartitions water between phases in the TTL, but has been largely overlooked. When clear, moist, stratified air is pushed upward above rising deep convection, it cools adiabatically, and the activity of solution aerosols in the air sometimes increases to the point that they freeze. The particles subsequently grow by the diffusion of water vapor to their surface, forming a tenuous veil over the tops of convective cloud turrets. These clouds have been called pileus, from the Latin word for the felt caps that were worn by freed slaves. They are termed "accessory clouds" because their formation requires prior existence of cloud of another genus.

The motivation for studying these clouds (or any other at such cold temperatures) is that, whenever molecules of water are converted from vapor to ice there is the potential for precipitation and a corresponding dessication of the air. Moreover, molecular

dipoles in close proximity vibrate in phase, so through condensation the interactions of water with terrestrial and solar radiation are greatly amplified. With this in mind, we detail some of the physical processes behind pileus formation through photography, in situ measurements, and numerical simulations, and conclude with a discussion of how they irreversibly redistribute water between phases in the TTL.

2 Photography

We show two examples of pileus clouds forming near the tropopause. The first shows pileus forming in "stacked" layers above a deep convective storm that developed over land in the Tropical Western Pacific region near Darwin, Australia (12° S, 130° E) (Fig. 1). While cloud top could not be determined in this case, a sounding from earlier in the day showed the tropopause was located near 18 km at 186 K. Fifteen minutes after this photograph was taken there was extensive lightning, an unusually intense surface gust front of 83 km hr^{-1}, a temperature drop of 10°C, and the precipitation intensity reached 80 mm hr^{-1}. While it is impossible to say with certainty, the vigor of the storm implies that the convection reached the tropopause near the time the photograph was taken. A photograph taken of the entire storm (not shown) indicates the system was nearly 100 km across, and suggests that the pileus formed in the lower stratosphere, extending about 2 km above the tropopause.

A second example is shown in Fig. 2, taken over Louisiana at an altitude of 12 km. Well above turbulent cirrus anvil outflow spreading from deep convection, two thinner stratiform cloud layers were seen. The higher of these layers showed wave-like features with a wavelength similar to the width of a turret of deep convection immediately below, which suggests the cirrus had been forced by the convection. The lower layer enveloped the turret in the characteristic skullcap veil of pileus. Six minutes later, the lower stratiform layer had been punctured by the turret, and it began to spread laterally above the anvil. There have been similar observations to these cited in Cameroon and Kenya by Lacaze (1966) and Scorer (1972).

The photographs show that pileus clouds can form at cold temperatures and low latitudes. Depending on its vertical extent and velocity, overshooting deep convection can puncture a pileus cloud it forms, in which case the pileus spreads laterally over the anvil cirrus beneath it.

3 A mixing process

Because convection is turbulent, it will mix with its surroundings. In the absence of a pileus layer, surrounding air would be subsaturated. Although the humidity might became enhanced around the convective cloud due to mixing (Perry and Hobbs, 1996; Lu et al., 2002), there would remain a sharp visual interface between the cloud and its environment. This process was illustrated in model simulations by Wang and Key (2003), in which interfacial turbulent mixing was generated by shear between the cloud and its environment (Grabowski and Clark, 1991, 1993). Alternatively, if a pileus cloud forms, and it is punctured by convection from below, ice mixed from the convection into its surroundings will not evaporate because the environment is supersaturated. Correspondingly, the pileus layer becomes enriched with water.

Examples of mixing between deep convection and cirrus that formed at the TTL were observed obtained from the NASA WB-57F aircraft during the July 2002 CRYSTAL-FACE campaign over Southern Florida and near Honduras (Garrett et al., 2004). Measurements of ice concentrations were obtained with a Cloud and Aerosol Particle Spectrometer (CAPS) (Baumgardner et al., 2002), water vapor and total water concentrations with the Harvard Water Probe (Weinstock et al., 1994), water isotopes with the Aircraft Laser Infrared Absorption Spectrometer (ALIAS) (Webster et al., 1994), and temperature and wind speed from the Meteorological Measurement System (MMS) (Scott et al., 1990).

Garrett et al. (2004) showed that cirrus in the TTL were commonly located directly above anvil outflow from deep convection. In these cases, the anvil and TTL cirrus were not formed independently, as is normally assumed. Rather, the TTL cirrus had nearly

the same horizontal dimensions as the anvil. Mixing ratios of nitrogen oxide (NO) and total water in the TTL cirrus were intermediate to those observed in clear TTL air and those in anvil cirrus. In one case, spectral analysis of the temperature field showed that the TTL cirrus contained a distinct gravity wave signature not seen in surrounding clear air, with a horizontal wavelength characteristic of deep convective turrets, and a vertical velocity and displacement amplitude of $\sim 3\,m\,s^{-1}$ and 300 m, respectively. These data suggested that much of the TTL cirrus observed during CRYSTAL-FACE originated as pileus that had mixed with the deep convection. The fractional contribution of deep convective air to TTL cirrus ranged up to 0.5.

The extent of mixing of different airmasses can be inferred from measurements of water isotopes, since these fractionate according to their condensation temperature – a proxy for their altitude (Kuang et al., 2003; Webster and Heymsfield, 2003). According to Rayleigh distillation, atmospheric water becomes progressively lighter as an air parcel is cooled; heavier isotopes preferentially condense and precipitate. In the absence of any mixing, the depletion of HDO relative to H_2O (δ-HDO) would range from −86 per mil above the ocean, to approximately −950 per mil at the coldest tropical tropopause. Recent measurements have shown average values of δ-HDO in the TTL are in fact near −640 per mil, which argues that the origins of TTL moisture are determined by condensation processes well below the tropopause (Kuang et al., 2003). However, Webster and Heymsfield (2003) showed that this value is only an average, and TTL values of δ-HDO are actually highly variable, ranging from −900 to ∼0 per mil at horizontal scales down to ∼3 km.

An example of such variability from CRYSTAL-FACE is shown in Fig. 3, from a vertical descent by the WB-57F through TTL cirrus followed by anvil cirrus. Values of both δ-HDO and total water concentrations in the TTL cirrus were intermediate to those seen in surrounding TTL air and anvil cirrus below. The implication is that the TTL cirrus had formed through some small-scale mechanism that mixed the TTL with convective air. This could have been where a pileus layer was punctured by deep convection. If a pileus cloud formed and spread, but was not punctured, δ-HDO in the TTL would have

remained unchanged; or, if TTL cirrus was derived entirely from anvil ejecta, δ-HDO in the layer would be close to zero. Figure 3 shows that δ-HDO is intermediate to these two values, which suggests that deep convection exchanged air with a TTL cirrus layer it forced. Additionally, the TTL cirrus is colder than its surroundings by about 3 K, which would be expected from an enthalpy exchange with cold overshooting deep convection.

4 Simulations

We are aware of no detailed description of the dynamics of pileus formation. As a guide, dimensional analysis suggests that by squeezing stratified isentropes upward, deep convection adiabatically cools the air it displaces by

$$\delta T \sim \frac{gW}{c_p N} \tag{1}$$

where g is gravity, c_p the heat capacity of dry air, N the buoyancy frequency of the TTL and W the vertical velocity of the convection. Values of W in deep convection commonly reach $\sim 10\,m\,s^{-1}$. However, above the base of the TTL, overshooting turrets decelerate rapidly so W should be somewhat smaller. An estimate of the cooling this forces is of order several degrees (Eq. 1). Condensate forms if this cooling is sufficient to raise the saturation ratio with respect to ice S_i to approximately 1.6 (Koop et al., 2000; Baker and Baker, 2004). Above this level, the amount of condensate that forms is determined by the Clausius-Clapeyron relation. To first order, it increases linearly with height.

A second consideration is the extent of wind shear. We speculate that if the Richardson number Ri in the TTL is low, a laminar pileus cloud will not form because buoyant stratification is insufficient to inhibit shear driven turbulence. Alternatively, wind shear may prohibit gravity waves from propagating vertically to a depth necessary to form pileus. Deep convection may form instead “anvil sheet plumes” or “overshooting plumes”, of the sort simulated by Wang and Key (2003) above a Great Plains storm.

Yamamoto et al. (2003) showed that, in a 1 km layer above the tropical temperature minimum, Ri is usually less than 0.5, and sometimes less than the "critical" turbulent value of 0.25, but that elsewhere the TTL is very stable. Lane et al. (2001) used numerical and analytical arguments to show that wind shear is a negligible source of waves around tropical convection, even where the deep convection penetrates a shear layer. Rather, the source of gravity waves can be understood primarily as due to the vertical oscillation of convective turrets about their level of neutral buoyancy (LNB) as they move with the wind.

4.1 Model description

To obtain a more detailed understanding of pileus formation, we have simulated numerically some of the more important physics involved, including forced cooling, homogeneous freezing of solution aerosol, ice crystal diffusional growth, and mixing with deep convection. Our model simulates the evolution of 2000 individual sulfuric acid solution particles within a parcel of clear TTL air. Consistent with measurements in the TTL (Lee et al., 2003), the size distribution of dry particles is log-normal and bimodal, with mode radii, spectral widths, and concentrations of 0.015 μm and 0.06 μm; 1.4 and 1.5; and 2500 cm^{-3} and 150 cm^{-3}, respectively. The parcel oscillates vertically with a frequency ω and a vertical velocity amplitude W. Being a parcel model, environmental wind shear is ignored.

Convection produces dispersive waves covering a wide spectrum in frequency and energy. We choose the most relevant frequency for cloud formation based on "stationary-phase" solutions to an initial value problem for the temporary displacement of stratified air (Lighthill, 2001): the highest frequency waves approaching the buoyancy frequency N have the largest vertical amplitude and therefore are most likely to produce the cooling required for cloud formation.

At equilibrium, solution aerosol adjust their volume V such that the solution activity a_w is equivalent to the relative humidity in surrounding air. Quasi-equilibrium is maintained, in spite of any influence of aerosol composition on surface kinetics (as argued

by Kärcher and Koop, 2005). This is because the diffusional time scale τ_{diff} is of order r^2/D, where r is the aerosol radius and D the diffusivity, which can be modified to account for kinetic limitations associated with molecular diffusion to small droplets. Even if the condensation coefficient for water molecule uptake is very low, τ_{diff} is many orders of magnitude less than the time scale associated with changes in ambient humidity: the aerosol is always effectively in equilibrium with its environment (Pruppacher and Klett, 1997).

The nucleation rate of ice embryos in solution $J(a_w, T)$ determines the probability $P = 1 - \exp(-JV\Delta t)$ an aerosol freezes in time period Δt (Koop et al., 2000; Baker and Baker, 2004). According to this formulation, aerosol freeze when the saturation ratio with respect to ice S_i reaches ~1.6. Large aerosol have the highest probability of freezing ($V \sim r^3$), but smaller aerosol tend to have correspondingly high concentrations ($N_a \sim r^{-3}$). Therefore, it is almost equally likely that aerosol of a given size will homogeneously freeze during Δt.

Once frozen, aerosol grow rapidly by vapor diffusion. This depletes the ambient vapor field and therefore a_w; further nucleation is suppressed and only a fraction of available aerosol become ice crystals. The assigned value of the condensation coefficient is 0.2 (Delval and Rossi, 2004). High ice crystal concentrations are favored by low T and high W, and are only weakly related to the size distributions of the aerosol (Kärcher and Lohmann, 2002).

The model permits mixing at the interface between pileus and deep convective cloud. At the apex of the first cycle in the wave, it is assumed this mixing occurs instantaneously. Sensible heat, vapor and ice are mixed linearly: i.e.,

$$\chi_{mixture} = (1 - f)\,\chi_{pileus} + f\,\chi_{convection}$$

where, χ is the mixed quantity and f the fraction mixed in from the convection. The model then tracks the sizes of individual particle as they adjust to instantaneous (in the case of haze) and diffusive (in the case of ice) equilibration with the rapid temperature fluctuations induced by convection.

4.2 Initialization

Unfortunately, no in situ airborne measurements are available of TTL pileus with which to initialize the model. Instead we use measurements of TTL cirrus and deep convective cloud sampled during straight northbound flight off the coast of Honduras on 9 July 2002 at an approximate altitude of 15 km.

Figure 4 shows a situation where deep convective cloud had punctured much more tenuous cirrus at the tropopause. The back-seater on the aircraft noted that flight was primarily through very tenuous cloud with a cirrus shield below. The deep convective cloud sampled at 67350 and 67800 s UTC had δ-HDO values close to zero with ice mixing ratio values approaching several hundreds ppmv; surrounding TTL cirrus was characterized by δ-HDO values of $\sim$−500 per mil and ice mixing ratio values typically less than 10 ppmv.

Wavelike fluctuations in zonal wind (U) and T were found in WB-57F MMS data between 67700 and 68300 s UTC within a 15.0 to 15.3 km layer. The initial encounter with a convective plume at 67800 s UTC was associated with a temperature drop of $\sim$3 K. As convective air was colder than its surroundings, the convective plume had risen above its LNB, locally squeezing isentropes upward. Two subsequent temperature drops ranged from 1.5 to 2.2 K, but were not within dense cloud. As such, these latter fluctuations represent gravity wave motions forced by the convection, with the strongest within the decelerating plume itself. Nearly constant temperature during a climb after 68300 s indicates the environment was locally isothermal.

Because the tropopause altitude was at $\sim$15 km, the aircraft sampled near the forcing level for the wave field. Near their source, the phase planes of gravity waves lie quasi-orthogonal to the mean wind vector (in this case U=11 m/s, V=0 m/s) at the forcing altitude. At 67930 utsec, 100 s period (in flight time) oscillations in U and T appear to be almost in phase, whereas at other times there appears to be no particular correlation. This suggests waves were propagating up and away from the convection, but at a frequency close to that required for decaying waves (Dean-Day et al., 1998). Because

a low-stability region overlaid the convection at 16 km altitude, wave reflection may also have influenced the degree of correlation.

The NASA ER-2 flew in stacked formation with the WB-57F over the same track, releasing a dropwindsonde approximately 250 km south-southeast of the convective cell, and less than 30 min prior sampling of the wave. The pressure-weighted mean wind, computed from the ocean surface (1006 mb) up to the tropopause at $\sim$135 hPa, was from the east-southeast at 6.2 m s^{-1}. Assuming the convection was advected with the deep layer mean wind, and considering the WB-57F traveled with a ground speed of $\sim$193 m/s on a northwestward track, the observed 100 s period oscillations seen in U correspond to a horizontal wavelength of 7.3 km. The static stability at the flight level corresponded to a buoyancy frequency of N=0.0164 s^{-1}. Accordingly, linear gravity wave theory predicts that the minimum wavelength and intrinsic frequency for propagating gravity waves was 4.2 km and 0.015 s^{-1}, respectively, which implies the observed waves were close to the decay criteria for vertical energy propagation.

Because of the damping effect of the aircraft mass, MMS vertical winds are most responsive at shorter observed periods (<50 s). Since we are investigating somewhat longer periods, we instead estimate the updraft velocity of the wave from linear wave theory. Assuming convection initially displaced the air parcel from equilibrium by 300 m, for a wave with an observed 100 s period moving westward at $\sim$6.2 m s^{-1}, a transit time of 3.5 min is required to move air from the warm to the cold phase. Thus, the wave's average updraft velocity W was $\sim$3 m s^{-1}. These results are consistent with others outlined by Garrett et al. (2004), which argue that the dynamics of TTL cirrus are driven by high frequency waves with an amplitude and wavelength consistent with forcing from uplift of the TTL by a turret of deep convection.

Based on the above discussion, and the measurements in the TTL cirrus shown in Fig. 4, the parcel model is intialized to values of S_i and T of 1.2 and 198 K, respectively. Convective air is assumed to be 3 K colder than its surroundings, with an ice mixing ratio of 150 ppmv and values of r_e=5 μm. Values of r_e obtained with the CAPS probe were in very close agreement with those obtained simultaneously using independent

measurement techniques (Garrett et al., 2003). Additionally, the gravity wave forced by the convection is assumed to have an amplitude of $4\,m\,s^{-1}$ and a frequency of $0.015\,s^{-1}$.

4.3 Results

Two cloud formation scenarios are modeled (Fig. 5). In the first, a pileus cloud forms when the parcel cools to the point that $S_i \simeq 1.6$. The pileus cloud stays separate from the convection and does not mix (i.e. $f=0$). Following ice nucleation of haze aerosol, the simulated pileus ice crystals grow to $\sim 1\,\mu$m radius, S_i falls toward equilibrium. While the air parcel enters the warm phase of the gravity wave, it becomes subsaturated, and the pileus ice crystals sublimate entirely. In subsequent cycles of the wave, the cloud formation process is repeated. In reality, a progressively reduced amplitude due to the dispersive nature of the wave will probably restrict pileus formation to the initial impulse.

In the second scenario, the pileus cloud is punctured by water-laden deep convection, and the two clouds mix. This is parameterized with a value of $f=0.1$, since this was a typical value based on observations of convective cloud and thin cirrus during CRYSTAL-FACE described by Garrett et al. (2004). Following mixing, the air parcel does not become subsaturated in the lower phase of the gravity wave. This is because, as deep convection mixes with its surroundings, it contributes not just the water vapor contained in cold dry air (as suggested by Sherwood and Dessler, 2000) but water from large ice crystals as well. These ice crystals have a higher value of r_e than those in the pileus because they originated from warmer temperatures. (Garrett et al. (2005) noted significant concentrations of precipitation size ice crystals measured in a similar TTL cirrus cloud overlying an anvil during CRYSTAL-FACE). Because these particles sublimate along with the original pileus ice crystals, they provide a reservoir of water vapor that inhibits subsaturation in the warm phase of the newly formed wave cloud. The cloudy air mass that is derived from TTL air only ever partially sublimates, and the cloud is sustained over repeated wave cycles. The combined effective radius

of the pileus and convection ice crystals modeled for this scenario is $2\,\mu$m, which is in good agreement with observations shown in Fig. 5.

Based on these analyses, we show in Fig. 6a graphical illustration of how we believe pileus clouds form and evolve.

5 Discussion

While it is evident from Fig. 1 that pileus clouds can form in the tropical TTL, their actual incidence remains unknown. The likelihood of pileus formation at any location depends on three factors: the stratification of the atmosphere, the velocity of the forced uplift, and foremost, the humidity: higher values of S_i require less lifting by convection to initiate ice crystal nucleation.

In the tropics, at least, thin cirrus and regions of high S_i are highly correlated in the TTL, and are most common in regions where deep convection is active (Sandor et al., 2000; Dessler and Yang, 2003; Wu et al., 2005). To illustrate, Microwave Limb Sounder (MLS) measurements obtained during 1992 aboard the Upper Atmosphere Research Satellite (UARS) (Read et al., 2004) show that air is often supersaturated in the lower tropical TTL, but only rarely so aloft (Fig. 7). Deep convective updrafts are also higher in the lower TTL, simply because they are above their LNB. If we assume a typical value for W of $\sim 3\,m\,s^{-1}$ at this level, the associated uplift of the TTL above the convection should be of order 300 m. MLS data suggest that in this event, at tropical latitudes, 20% (10%) of lower TTL air over land (ocean) deep convection will see formation of pileus cloud.

We note that this estimate of pileus incidence is likely conservative because MLS values of S_i represent an average over a vertical depth of ~ 4 km, whereas high humidity layers are often thinner (and presumably more common). Also, convective updrafts, and corresponding displacements of stratified air above, are particularly high over land where humidities are highest. Finally, aircraft measurements off Honduras and Costa Rica show air mostly supersaturated into the middle TTL (Fig. 7, Jensen et al., 2005).

Onced formed, the impact of pileus clouds on distributions of water vapor and ice in the tropopause depends in large part on their longevity. Model results show that pileus ice crystals are very small, only several micrometers across, in which case their lifetimes under gravitational settling is of order 10 days. However, ordinarily it would be expected that the cloud would exist only in the phase of the gravity wave where S_i>1. Once the potential energy associated with the vertical displacement of the initial impulse has dispersed, it might be expected that the cloud will disappear.

Nonetheless, there are suggestions that these clouds can be relatively long-lived. Observations from CRYSTAL-FACE showed that TTL cirrus above anvils appears to begin as pileus, it is stable, and it does not dissipate where the anvil beneath it does (Garrett et al., 2004, 2005). Comstock et al. (2002) noted a similar example in the TWP with the TTL cirrus lasting for days after the initial convective event.

There are several reasons why this might be the case. In the lower troposphere, at temperatures above the homogeneous freezing temperature of about 235 K, wave cloud both forms and evaporates at the same relative humidity, i.e. at 100% with respect to water. The cloud forms from initially subsaturated air, but once the forcing mechanism dissipates, the cloud disappears. In the TTL, however, it appears that pileus clouds can only form when the initial value of S_i is supersaturated (Fig. 7). Because clear air may initially have values of S_i>1, when uplift forms a pileus layer, the cloudy air may persist even following dissipation of the initial disturbance, and relaxation of S_i to its initial value.

A further consideration is that, because pileus cloud can spread above the anvil, it is shielded from evaporation due to terrestrial heating from below. It has been suggested by Hartmann et al. (2001) and demonstrated by Garrett et al. (2005) that the presence of a cold anvil layer beneath in fact encourages cooling of TTL cirrus that is formed.

We also showed that the pileus longevity can be sustained by mixing with the deep convection itself. Overshooting deep convective clouds may be dry compared to their warmer surroundings, but they are also laden with water in the form of ice; their tops would not be clearly visible otherwise. Because convection is turbulent, it necessarily

mixes into its surroundings both water vapor and the ice. If the environment is subsaturated, the ice evaporates where we normally interpret the edge of the cloud to exist, leaving behind a halo of humid air. If the environment is supersaturated, however, a pileus cloud will form ahead of the convection; when the pileus is punctured, ice crystals are mixed from the convection into a cloudy atmosphere and do not completely evaporate. In fact, these ice crystals act as a reservoir of water vapor that inhibit subsaturation in the warm phase of ensuing buoyancy oscillations of the pileus cloud. While these larger ice crystals of convective origin may eventually precipitate, cloud has been irreversibly formed within the fraction of the mixed air that was derived from the previously clear TTL.

Thus, rather than being merely an ephemeral curiosity, pileus clouds may influence how both ice and water are distributed and partitioned in the TTL. Any redistribution is tied to deep convection through small scale processes at altitudes well above the convective level of neutral buoyancy where anvil cirrus is normally found. Space-borne measurements of the TTL with lidar and radar should help show where and how often thin cirrus are present above deep convection. Detailed cloud resolving model simulations might show how these clouds evolve.

Acknowledgements. The authors gratefully acknowledge support from NASA Grants NAG511505 and NNG045I68G, S. Fueglistaler for discussions, E. Weinstock for measurements of water vapor, M. Kimball for drafting Fig. 6, and the contributions of the flight crew of the NASA WB-57F aircraft.

References

Baker, M. B. and Baker, M.: A new look at homogeneous freezing of water, Geophys. Res. Lett., 31, L19102, doi:10.1029/2004GL020483, 2004. 8214, 8216

Baumgardner, D., Jonsson, H., Dawson, W., O'Connor, D., and Newton, R.: The cloud, aerosol and precipitation spectrometer (CAPS): A new instrument for cloud investigations, Atmos. Res., 59–60, 251–264, 2002. 8212

Comstock, J. M., Ackerman, T. P., and Mace, G. G.: Ground-based lidar and radar remote sensing of tropical cirrus clouds at Nauru Island: cloud statistics and radiative impacts, J. Geophys. Res., 107, 4714, doi:10.1029/2002JD002203, 2002. 8221

Dean-Day, J., Chan, K. R., Bowen, S. W., Bui, T. P., Gary, B. L., and Mahoney, M. J.: Dynamics of Rocky Mountain lee waves observed during SUCCESS, Geophys. Res. Lett., 9, 1351–1354, 1998. 8217

Delval, C. and Rossi, M. J.: The kinetics of condensation and evaporation of H_2O from pure ice in the range 173–223 K: a quartz crystal microbalance study, Phys. Chem. Chem. Phys., 6, 4665–4676, doi:10.1039/b40995h, 2004. 8216

Dessler, A. E. and Yang, P.: The distribution of tropical thin cirrus clouds inferred from Terra MODIS data, J. Climate, 16, 1241–1247, 2003. 8220

Garrett, T. J., Gerber, H., Baumgardner, D. G., Twohy, C. H., and Weinstock, E. M.: Small, highly reflective ice crystals in low-latitude cirrus, Geophys. Res. Lett., 30, 2132, doi:10.1029/2003GL018153, 2003. 8219

Garrett, T. J., Heymsfield, A. J., Ridley, B. A., McGill, M. J., Baumgardner, D. G., Bui, T. P., and Webster, C. R.: Convective generation of cirrus near the tropopause, J. Geophys. Res., 109, D21203, doi:10.1029/2004JD004952, 2004. 8212, 8218, 8219, 8221

Garrett, T. J., Navarro, B. C., Twohy, C. H., Jensen, E. J., Baumgardner, D. G., Bui, P. T., Gerber, H., Herman, R. L., Heymsfield, A. J., Lawson, P., Minnis, P., Nguyen, L., Poellot, M., Pope, S. K., Valero, F. P. J., and Weinstock, E. M.: Evolution of a Florida cirrus anvil, J. Atmos. Sci., 62, 7, 2352–2372, doi:10.1175/JAS3495.1, 2005. 8219, 8221

Grabowski, W. W. and Clark, T. L.: Cloud-environment interface instability: Rising thermal calculations in two spatial dimensions, J. Atmos. Sci., 48, 527–546, 1991. 8212

Grabowski, W. W. and Clark, T. L.: Cloud-environment interface instability, part II: Extension to three spatial dimensions., J. Atmos. Sci., 50, 555–573, 1993. 8212

Hartmann, D. L., Holton, J. R., and Fu, Q.: The heat balance of the tropical tropopause, cirrus, and stratospheric dehydration, Geophys. Res. Lett., 28, 1969–1972, 2001. 8221

Jensen, E. J., Smith, J. B., Pfister, L., Pittman, J. V., Weinstock, E. M., Sayres, D. S., Herman, R. L., Troy, R. F., Rosenlof, K., Thompson, T. L., Fridlind, A. M., Hudson, P. K., Cziczo, D. J., Heymsfield, A. J., Schmitt, C., and Wilson, J. C.: Ice supersaturations exceeding 100% at the cold tropical tropopause: implications for cirrus formation and dehydration, Atmos. Chem. Phys., 5, 851–862, 2005,
SRef-ID: 1680-7324/acp/2005-5-851. 8220

Kärcher, B. and Koop, T.: The role of organic aerosols in homogeneous ice formation, Atmos. Chem. Phys., 5, 703–714, 2005,
SRef-ID: 1680-7324/acp/2005-5-703. 8216

Kärcher, B. and Lohmann, U.: A parameterization of cirrus cloud formation: Homogeneous freezing including effects of aerosol size, J. Geophys. Res., 107, 4698, doi:10.1029/2001JD001429, 2002. 8216

Koop, T., Luo, B., Tsias, A., and Peter, T.: Water activity as the determinant for homogeneous ice nucleation in aqueous solutions, Nature, 406, 611–614, 2000. 8214, 8216, 8232

Kuang, Z., Toon, G. C., Wennberg, P. O., and Yung, Y. L.: Measured HDO/H_2O ratios across the tropical tropopause, Geophys. Res. Lett., 30, 1372, doi:10.1029/2003GL017023, 2003. 8213

Lacaze, J.: Remarques sur les pileus, J. Rech. Atmos., 4, 487–488, 1966. 8211

Lane, T. P., Reeder, M. J., and Clark, T. L.: Numerical modeling of gravity wave generation by deep tropical convection, J. Atmos. Sci., 58, 1249–1274, 2001. 8215

Lee, S.-H., Wilson, J. C., Reeves, J. M., and Lafleur, B. G.: Aerosol size distributions from 4 to 2000 nm measured in the upper troposphere and lower stratosphere, in: European Aerosol Conference, Madrid, Spain, 2003. 8215

Lighthill, J.: Waves in fluids, Cambridge University Press, 2001. 8215

Lu, M., McClatchey, R. A., and Seinfeld, J. H.: Cloud halos: numerical simulation of dynamical structure and radiative impact, J. Appl. Meteor., 41, 832–848, 2002. 8212

Perry, K. D. and Hobbs, P. V.: Influences of isolated cumulus clouds on the humidity of their surroundings, J. Atmos. Sci., 53, 159–174, 1996. 8212

Pruppacher, H. R. and Klett, J. D.: Microphysics of Clouds and Precipitation, 2nd Rev. Edn., Kluwer Academic Publishing, Dordrecht, 1997. 8216

Read, W. G., Wu, D. L., Waters, J. H., and Pumphrey, H. C.: A new 147-56 hPa water vapor product from the UARS Microware Limb Sounder, J. Geophys. Res., 109, D06111, doi:10.1029/2003JD004366, 2004. 8220

Sandor, B. J., Jensen, E. J., Stone, E. M., Read, W. G., Waters, J. W., and Mergenthaler, J. L.: Upper tropospheric humidity and thin cirrus, Geophys. Res. Lett., 27, 2645–2648, 2000. 8220

Scorer, R.: Clouds of the World, Stackpole Books, 1972. 8211

Scott, S., Bui, T. P., Chan, K. R., and Bowen, S. W.: The meteorological measurement system on the NASA ER-2 aircraft, J. Atmos. Ocean. Technol., 7, 525–540, 1990. 8212

Sherwood, S. C. and Dessler, A. E.: On the control of stratospheric humidity, Geophys. Res. Lett., 27, 2513–2516, 2000. 8219

Wang, X. and Key, J. R.: Recent trends in Arctic surface, cloud, and radiation properties from space, Science, 299, 1725–1728, doi:10.1126/science.1078065, 2003. 8212, 8214

Webster, C. R. and Heymsfield, A. J.: Water isotope ratios D/H, $^{18}O/^{16}O$, $^{17}O/^{16}O$ in and out of cloud map dehydration pathways, Science, 302, 1742–1745, doi:10.1126/science.1089496, 2003. 8213

Webster, C. R., May, R. D., Trimble, C. A., Chave, R. G., and Kendall, J.: Aircraft (ER-2) laser infrared absorption spectrometer (ALIAS) for in-situ stratospheric measurements of HCl, N_2O, CH_4, NO_2, and HNO_3, Appl. Opt., 33, 454–472, 1994. 8212

Weinstock, E. M., Hintsa, E., Dessler, A., Oliver, J., Hazen, N., Demusz, J., Alien, N.T.and Lapson, L., and Anderson, J.: New fast response photofragment fluorescence hygrometer for use on the NASA ER-2 and the Perseus remotely piloted aircraft, Rev. Sci. Instrum., 65, 3544–3554, 1994. 8212

Wu, D. L., Read, W. G., Dessler, A. E., Sherwood, S. C., and Jiang, J. H.: UARS/MLS cloud ice measurements: implications for H_2O transport near the tropopause, J. Atmos. Sci., 62, 518–530, 2005. 8220

Yamamoto, M. K., Fumiwara, M., Horinouchi, T., Hashiguchi, H., and Fukao, S.: Kelvin-Helmholtz instability around the tropical tropopause observed with the Equatorial Atmosphere Radar, Geophys. Res. Lett., 30, 1476, doi:10.1029/2002GL016685, 2003. 8215

Fig. 1. Photo of pileus forming on top of deep convection over land near Darwin, Australia on 14 November 2004 at 7:05 p.m. local time. Although no radar measurements were made of cloud top, at 9:30 a.m., the tropopause was located at 17.8 km and −87°C (186 K). Precipitation rates at the Darwin ARM site reached 80 mm hr^{-1}, and wind gusts reached 83 km hr^{-1} at the Darwin airport just 15 min later.

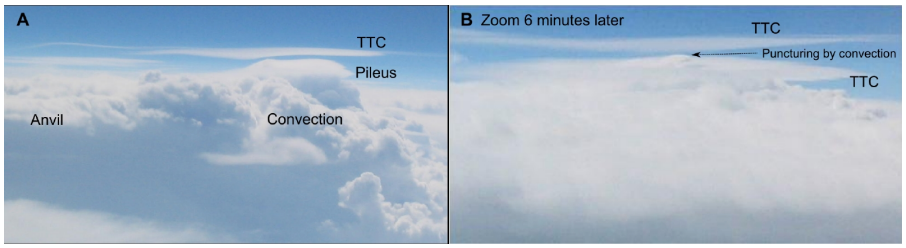

Fig. 2. Photographs of pileus and thin cirrus formation obtained at 12 km altitude over Louisiana on 30 April 2004 during the Mid-Latitude Cirrus Experiment (MidCiX). Photograph **(B)** is a closeup of the convective dome shown 6 min earlier in **(A)**.

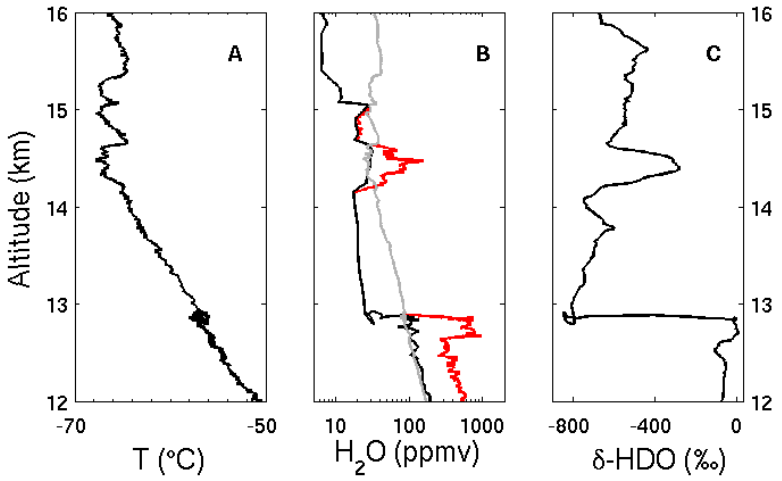

Fig. 3. Profile of **(A)** temperature, **(B)** H_2O mixing ratios (measured vapour: black; saturation vapour with respect to ice: grey; total (vapour plus ice: red) and δ–HDO in a profile obtained on 28 July 2002 over southern Florida. Two isotopically distinct cloud layers are seen: anvil cirrus outflow from convection located below 13 km altitude, and a more tenuous TTL layer centered at 14.5 km altitude. Values of δ-HDO in the anvil indicate it originated from lower tropospheric air. In the TTL cloud, values of δ-HDO and H_2O are intermediate to those in the anvil and TTL. The implication is that the TTC formed from a mixing process between surface and TTL airmasses.

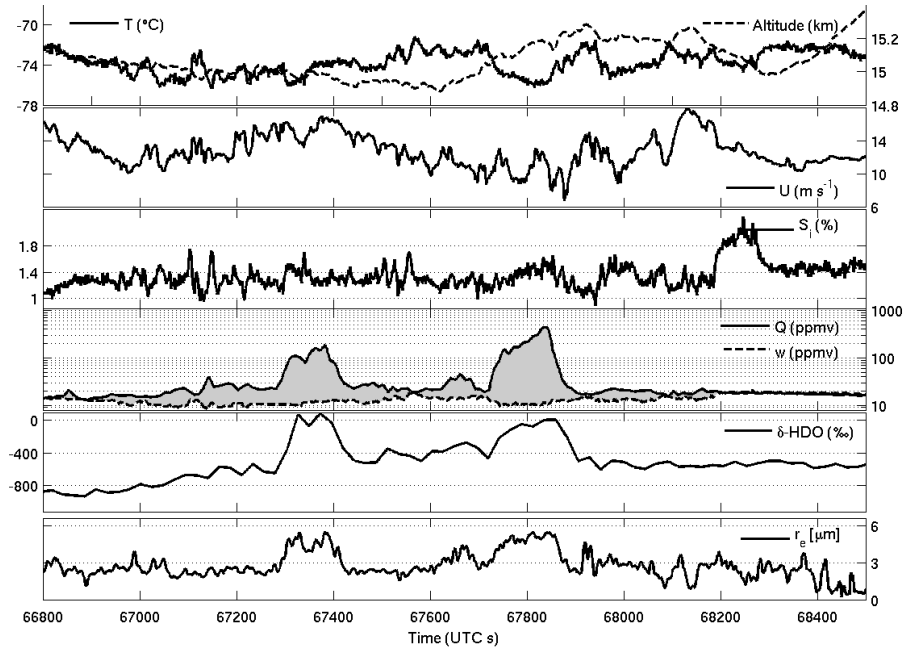

Fig. 4. Flight transect through cloudy air at approximately 15 km altitude off the East coast of Honduras. Measurements show temperature T, altitude, zonal wind velocity U, saturation ratio with respect to ice S_i, total Q and vapor w water mixing ratios, fractionation of HDO relative to H_2O $\delta-$HDO, and ice crystal effective radius r_e. Shaded area shows mixing ratios of ice.

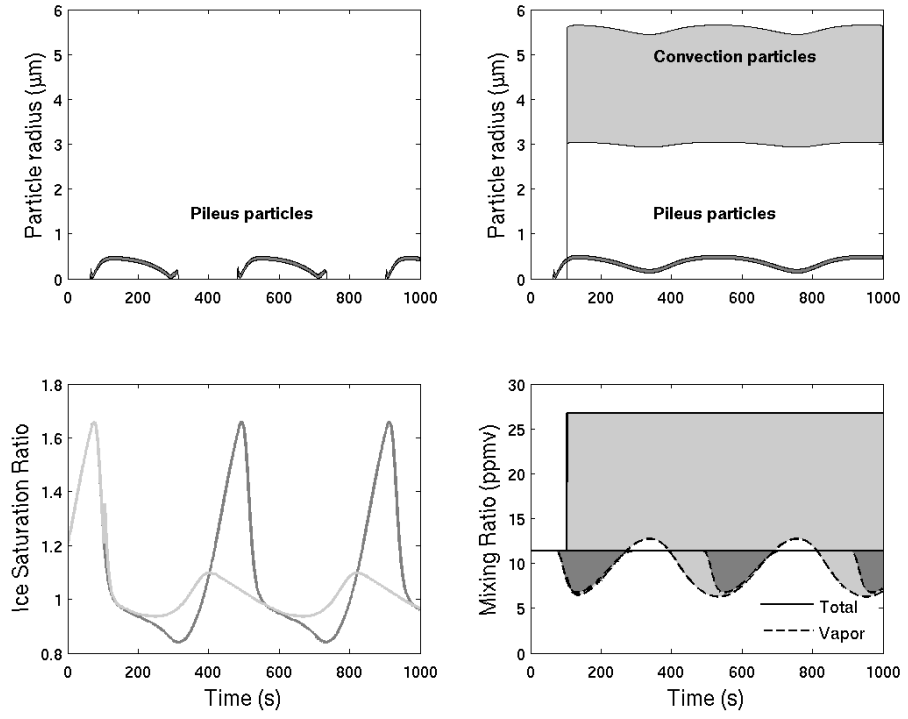

Fig. 5. Simulations of pileus cloud formation under scenarios of no mixing (dark gray), and mixing with a deep convective cloud turret (light gray). The shaded area represents the condensed phase (total water minus vapor).

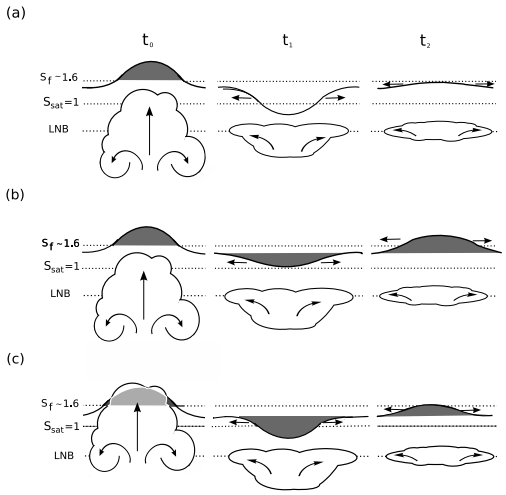

Fig. 6. A schematic diagram showing the hypothesized formation of a pileus cloud and its evolution through successive phases of the ensuing gravity wave. **(a)** An initially flat isentropic surface has a value of S_i greater than unity (S_{sat}) but below the homogeneous freezing point S_f, were it to be lifted adiabatically. Vertical perturbation of the surface causes a cloud to form above the point where it reaches S_f. In the warm phase of the wave, however, the cloud evaporates where it dips below S_{sat}. The cloud does not reform because the wave energy propagates, diminishing the wave amplitude in subsequent cycles. **(b)** The same as (a), but the cloud never evaporates because the wave never warms sufficiently to evaporate the cloud. **(c)** Deep convection punctures, then mixes with the pileus cloud. Ice crystals are exchanged through turbulent mixing at the interface between the two clouds. The added water enables the pileus cloud to survive the warm phase of the gravity wave, even where it dips below the level normally associated with S_{sat} in the absence of mixing. Note that this diagram illustrates only individual pulses of convective thermals and pileus, and not rather a continued sequence of impulses that blend together as they spread.

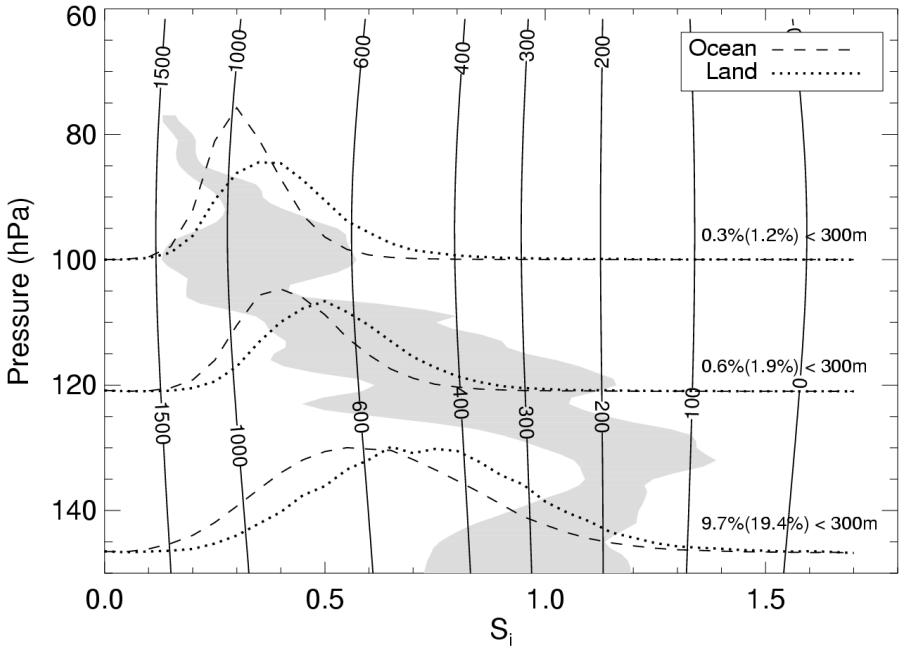

Fig. 7. Distributions of S_i in the tropical TTL retrieved 20° S and 20° N using Version 7.02 Microwave Limb Sounder (MLS) measurements aboard the UARS satellite (lines), and in situ from two flights off Honduras flown during the July 2002 CRYSTAL-FACE project (shaded area). Contours represent the estimated isentropic lifting (in meters) required to initiate freezing at that level (Koop et al., 2000). At 146 hPa, assuming deep convection lifts air by 300 m, ~20% (10%) of land (ocean) air will form pileus cloud. The uncertainty in MLS S_i is approximately 30%, 40% and 50% at 146 hPa, 121 hPa, and 100 hPa, respectively.